Available online at www.sciencedirect.com
ScienceDirect
Geochimica et Cosmochimica Acta 74 (2010) 3913–3924
Geochimica et Cosmochimica Acta
www.elsevier.com/locate/gca

Tracing mechanisms controlling the release of dissolved silicon in forest soil solutions using Si isotopes and Ge/Si ratios

J.-T. Cornelis [a,*], B. Delvaux [a], D. Cardinal [b], L. André [b], J. Ranger [c], S. Opfergelt [a]

[a] Earth and Life Institute, Université catholique de Louvain, Croix du Sud 2/10, 1348 Louvain-la-Neuve, Belgium
[b] Dept. of Geology and Mineralogy, Royal Museum for Central Africa, Leuvensesteenweg 13, B-3080 Tervuren, Belgium
[c] Biogeochemistry of forest ecosystem, INRA Centre de Nancy, 54280 Champenoux, France

Received 23 October 2009; accepted in revised form 23 April 2010; available online 6 May 2010

Abstract

The terrestrial biogenic Si (BSi) pool in the soil–plant system is ubiquitous and substantial, likely impacting the land-ocean transfer of dissolved Si (DSi). Here, we consider the mechanisms controlling DSi in forest soil in a temperate granitic ecosystem that would differ from previous works mostly focused on tropical environments. This study aims at tracing the source of DSi in forest floor leachates and in soil solutions under various tree species at homogeneous soil and climate conditions, using stable Si isotopes and Ge/Si ratios. Relative to granitic bedrock, clays minerals were enriched in ^{28}Si and had high Ge/Si ratios, while BSi from phytoliths was also enriched in ^{28}Si, but had a low Ge/Si ratio. Such a contrast is useful to infer the relative contribution of silicate weathering and BSi dissolution in the shallow soil on the release of DSi in forest floor leachate solutions. The $\delta^{30}Si$ values in forest floor leachates ($-1.38‰$ to $-2.05‰$) are the lightest ever found in natural waters, and Ge/Si ratios are higher in forest floor leachates relative to soil solution. These results suggest dissolution of ^{28}Si and Ge-enriched secondary clay minerals incorporated by bioturbation in organic-rich horizons in combination with an isotopic fractionation releasing preferentially light Si isotopes during this dissolution process. Ge/Si ratios in soil solutions are governed by incongruent weathering of primary minerals and neoformation of secondary clays minerals. Tree species influence Si-isotopic compositions and Ge/Si ratios in forest floor leachates through differing incorporation of minerals in organic horizons by bioturbation and, to a lesser extent, through differing Si recycling.

1. INTRODUCTION

Silicon (Si) is the second most abundant element of the Earth's crust (Wedepohl, 1995) and the dominant solute in rivers draining continents (Gaillardet et al., 1999). It is well established that rooted vascular plants greatly influence the terrestrial Si cycle through silicate weathering by modifying the pH value (Kelly et al., 1998; Berner, 1997) and through Si recycling (Bartoli, 1983; Alexandre et al., 1997; Cornelis et al., 2010). In a forest ecosystem, trees take up a substantial amount of monosilicic acid ($H_4SiO_4^0$) from soil solution (Bartoli, 1983; Lucas et al., 1993; Alexandre et al., 1997; Lucas, 2001; Hodson et al., 2005; Cornelis et al., 2010). $H_4SiO_4^0$ is translocated to transpiration sites where it polymerizes as biogenic opal called phytoliths (Jones and Handreck, 1965) generating a significant and ubiquitous terrestrial biogenic silica (BSi) pool (Conley, 2002; Sommer et al., 2006; Henriet et al., 2008). The soil–tree system may impact on the land-ocean Si flux, which currently contributes to more than 80% of the dissolved Si (DSi) input to the oceans (Tréguer et al., 1995). Accordingly, the Si soil–tree cycle might play a major role in the global climate on a geological timescale. Indeed, the interactions between Si and C cycles regulate the atmospheric carbon dioxide through diatoms' productivity in the oceans

* Corresponding author. Tel.: +32 10 47 36 38; fax: +32 10 47 45 25.
E-mail address: jean-thomas.cornelis@uclouvain.be (J.-T. Cornelis).

0016-7037/$ - see front matter © 2010 Elsevier Ltd. All rights reserved.
doi:10.1016/j.gca.2010.04.056

(Smetacek, 1999) and weathering processes on the continents (Volk, 1987; Berner, 1997; Sommer et al., 2006).

As suggested by Basile-Doelsch (2006), Si can be considered as being distributed in two main pools: a primary Si-I pool (crystalline rocks and their sedimentary detrital derivatives) and a secondary Si-II pool that leaves the Si-I pool by weathering producing secondary precipitates. On continents, $H_4SiO_4^0$ is released in soil solutions where its concentration is principally influenced by mineral weathering, plant uptake, secondary clay mineral formation, adsorption onto oxides and leaching to the hydrosphere. The dissolution of litho- and pedogenic minerals as well as biogenic minerals contributes to the pool of DSi in soil solutions exported to the rivers.

Germanium (Ge) is a trace element, which is often considered as an analog to Si due to its very similar chemical properties (Azam and Volcani, 1981). The study of Ge/Si fractionation allows tracing silicate weathering and the biogeochemical cycle of Si (Kurtz et al., 2002; Derry et al., 2005; Scribner et al., 2006), as clay minerals and biogenic opal display contrasting Ge/Si ratios. Clay-sized weathering products are enriched in Ge (Murnane and Stallard, 1990; Kurtz et al., 2002; Kurtz and Derry, 2004) whereas phytoliths (BSi) are depleted in Ge relative to Si (Derry et al., 2005; Blecker et al., 2007; Delvigne et al., 2009).

Similarly, the fractionation of stable Si isotopes represents a useful tool to study the Si soil–plant cycle (Ziegler et al., 2005a; Engström et al., 2008; Opfergelt et al., 2010). The δ^{30}Si values in freshwater and seawater show enrichment in heavy Si isotope in comparison to δ^{30}Si values of magmatic and metamorphic rocks, suggesting isotopic fractionation during biogeochemical processes (De La Rocha et al., 2000; Ding et al., 2004; Alleman et al. 2005; Georg et al., 2006, 2007). The neoformation of secondary precipitates as clay minerals (Ziegler et al., 2005a,b; Opfergelt at al., 2008), plant Si uptake producing biogenic opal (Douthitt, 1982; Ziegler et al., 2005a; Ding et al., 2005, 2008; Opfergelt et al., 2006a,b, 2008), and adsorption of Si onto Fe-oxides (Delstanche et al., 2009; Opfergelt et al., 2009) are processes favoring the incorporation of light Si isotopes, generating rivers enriched in heavy Si isotopes (De La Rocha et al., 2000; Ding et al., 2004; Georg et al., 2006, 2007). Silicon isotope data alone can hardly decipher these three processes. Combining Ge/Si and Si isotope data may provide a better understanding of the Si pathways in a well-defined soil–tree system before its release in soil solution (Delvigne et al., 2009; Opfergelt et al., 2010; Lugolobi et al., 2010).

This study aims to assess the relative contribution of Si released from dissolution of primary and secondary minerals and from biogenic opal to soil solutions. For this purpose, δ^{30}Si and Ge/Si data are combined to investigate the soil–tree systems, which show similar acid-brown soils, climatic conditions and parental material but differ in the planted tree species. Silicon isotopic compositions and Ge/Si ratios were measured in (i) forest floor leachates and soil solutions, (ii) different soil fractions (bedrock; clay, silt, and sand fractions), and (iii) plant-related compartments of the forest ecosystem (plant BSi from phytoliths, and organic-rich horizons).

2. MATERIALS AND METHODS

2.1. Experimental site

The experimental site is located at Breuil-Chenue (Nièvre-Morvan, France, 47°18′10″N; 4°4′44″E), on a plateau at 638 m above sea level. The mean annual rainfall is 1212 mm and the mean annual temperature is 9 °C. According to the Köpper–Geiger climate map of Europe, the climate is Cfb, i.e. a temperate climate without dry season and with a warm summer (Peel et al., 2007). The parental material is the granite of "La Pierre-qui-Vire", which is covered by a thin layer of cryoturbated Quaternary loess (Aurousseau, 1976). The acid brown soil is classified as an Alumnic Cambisol (IUSS, 2006) and is developed from a granite with 34.5% quartz, 24% feldspars, 30.7% albite, 8.5% muscovite, 1.7% biotite and 0.6% chlorite leading to total concentrations of 0.1% MgO, 0.3% CaO, 1.3% Fe_2O_3, 3.5% K_2O, 3.5% Na_2O, 13.5% Al_2O_3 and 76.1% SiO_2 (Ranger et al., 2004; Mareschal, 2008). The soil was sandy–loamy (55% sands and <20% clays) and acidic (pH 3.8–4.6). Table 1 presents the major properties of the acid brown soil (Ranger et al., 2004). The native forest mixes trees dominated by European beech (*Fagus sylvatica* L.) and oak (*Quercus sessiliflora* Smith.). It was clear-cut in 1976 and replaced by six monospecific plantations. Out of these plantations, we selected five forest stands: Douglas fir (*Pseudotsuga menziesii* Franco), Norway spruce (*Picea abies* Karsten), Black pine (*Pinus nigra* Arn. *Ssp laricio* Poiret var corsicana.), European beech (*Fagus syslvatica* L.) and oak (*Quercus sessiliflora* Smith.). The Si contents of tree compartments, soils and solutions were presented by Cornelis et al. (2010).

2.2. Sampling and physico-chemical characterization

2.2.1. Soil and plant samples

The sampling was conducted in November 2006 and described in detail by Cornelis et al. (2010). Briefly, leaves and needles were collected from 5 litter traps per stand. Three replicates of forest floor horizons were sampled under each forest stand from which we have selected the fragmented (Of) and humified (Oh) horizons above the mineral soil layers. Moreover, three replicates of soil organo-mineral and mineral layers were sampled, under each forest stand, at the following systematic depths (cm) below the organic soil horizons: 0–7.5; 7.5–15; 15–30; 30–45; 45–60; 60–75. Solid

Table 1
Major characteristics of the acid brown soil under the 1976 native forest (Ranger et al., 2004).

Depth (cm)	pH (H_2O)	pH (KCl)	CEC[a] ($cmol_c\ kg^{-1}$)	C%	N%
0–5	3.8	3.2	9.2	7.4	0.39
5–10	4.2	3.7	6.9	4.0	0.21
10–15	4.5	4.0	5.1	2.3	0.17
15–25	4.6	4.2	4.0	2.4	0.13
25–40	4.5	4.3	3.0	1.5	0.08

[a] CEC, cation exchange capacity.

samples were then mixed to build up composite samples for each depth, and sieved at 2 mm to obtain the fine earth fraction (bulk soil <2 mm). Granitic bedrock buried in the soil profile was also collected from the experimental site. Soil physical and chemical properties were strictly identical between trees plots when the experimental site was set up (Bonneau et al., 1977). Thus, we assume homogeneous soils conditions between plots of monospecific plantations.

Tree BSi was extracted from leaves and needles after digestion of organic matter in an mixture of ultrapure concentrated HNO_3 (70%)/H_2O_2 (30%). In humus (Oh) and mineral soil layers, amorphous silica fraction (ASi), which includes BSi, was extracted both by gravimetric separation using heavy liquid for all forest stands and alkaline dissolution for Douglas fir, Black pine and European beech (Cornelis, 2010). The sand fraction [50–2000 μm] was separated from the fine earth fraction [<2 mm] by ultrasonic dispersion and wet sieving. Clay [0–2 μm] and silt [2–50 μm] fractions were then collected by gravimetric sedimentation (Rouiller et al., 1972). The separation of sand, silt and clay fractions was conducted on humus (Oh) and mineral soil layers, as it was shown that organic layers incorporated minerals from lower soil layers through bioturbation (Cornelis et al., 2010). Clay fractions, treated with Na-citrate at 100 °C, were saturated with K^+ and Mg^{2+} and clay minerals were identified by X-ray diffraction using CuKα radiation in a Bruker Advance diffractometer (at UCL) after saturation with ethylene glycol (EG) and heating (105, 300 and 550 °C) (Robert and Tessier, 1974).

2.2.2. Solution samples

In each forest stand, forest floor leachate solutions were collected in September 2008 by using two sets per forest stand of 9 lysimeters made of polypropylene (zero tension plate) placed just above the mineral soil (i.e. 0 cm). In addition, ceramic cup lysimeters were introduced into the soil profile at 60 cm depth and connected to a vacuum pump, which maintained a constant suction of −400 hPa to collect soil solutions (5 replicates per forest stand). The solutions were filtered at 0.45 μm and maintained at 4 °C.

Cations concentrations (Ca^{2+}, K^+, Na^+, Mg^{2+} and Mn^{2+}) in forest floor leachates and soil solutions were analyzed by inductively coupled plasma atomic emission spectrometry (ICP-AES). Anions concentrations (F^-, Cl^-, SO_4^{2-}, NO_2^-, NO_3^- and PO_4^{3-}) were measured by ionic chromatography (Dionex DX 300). The dissolved organic carbon (DOC) concentration was determined using a TOC-5050 Shimadzu. Concentrations represent the average of monthly measurements between April 2006 and April 2007, which were performed at the "Institut National de la Recherche Agronomique" (INRA-Champenoux, France).

2.3. Si and Ge analyses

Ge/Si ratios were determined from the Ge and Si concentrations in (i) granitic bedrock, (ii) sand, silt and clay fractions from the 30 to 45 cm mineral layer at European beech site, assuming soil homogeneity under each tree species, (iii) tree BSi, organic horizons (Of, Oh) above the mineral soil, bulk soils (0–7.5 and 30–45 cm) for the five forest stands, and (iv) forest floor leachates and soil solutions collected under the five forest stands.

Most Si and Ge analyses were performed by ICP-AES and inductively coupled plasma mass spectrometer (ICP-MS, Thermo Elemental X7), respectively, at the "Service d'Analyse des Roches et des Minéraux" (SARM, CNRS Nancy, France). Si and Ge were recovered after $LiBO_2$ fusion at 1000 °C in a Pt crucible (Carignan et al., 2001). Detection limits for Ge (0.05 μg g^{-1} for solid samples and 2 ng l^{-1} for solutions) were calculated as six times the standard deviation of the mean plus the mean of 150 procedure blanks for solids (borate fusion) and 10 solution blanks for solutions (HNO_3 2%). The accuracy was determining by measuring six reference rock and water standards (BR, AN-G, UB-N, DR-N, GH and SLRS-4; Carignan et al., 2001; Yeghicheyan et al., 2001). The Si reproducibility was better than 5% for rocks and solutions while the Ge reproducibility was better than 15% for rocks and better than 10% for aqueous solutions in the concentration ranges obtained.

Some solid samples (leaves and needles) with low Ge concentrations were analyzed by hydride-generation ICP-MS (PerkinElmer ELAN 6100 DRC) at the Ut2A-Pau (France) following the method adapted from Mortlock and Froelich (1996). Germanium was extracted on hot plate in nitric acid and hydrogen peroxide media. The acid extract was concentrated by evaporation to a 1 ml volume and then diluted with ultrapure water at 6 ml final volume. As no certified samples were available, the accuracy was checked by spiking a sample at 2 ng g^{-1} Ge in the solid sample (about 70 ng l^{-1} Ge in the extract). The detection limit for Ge was 0.05 ng g^{-1} and Ge reproducibility was better than 20%.

Germanium contents in clay minerals were measured by high resolution (HR) ICP-MS (Element 2) after borate fusion at 1000 °C for 1 h in Pt crucibles at the "Royal Museum for Central Africa" (RMCA, Belgium). Details about the method, reproducibility and accuracy are available in Delvigne et al. (2009).

2.4. Si isotope analyses

Two forest stands of contrasting tree species, Douglas fir (coniferous) and European beech (deciduous), were selected for Si isotope analyses because of the time-consuming sample preparation. The Si-isotopic compositions were determined on (i) granitic bedrock, (ii) bulk soils (0–7.5 cm, 30–45 cm), and separated sand, silt and clay fractions from the soil layer (30–45 cm) at the European beech site (iii) tree BSi and humus layers (Oh), and (iv) forest floor leachates. Silicon was recovered from solid sample material by alkaline fusion at 1000 °C. Five milligrams of sample were mixed with 30 mg of $LiBO_2$ flux in a covered Pt crucible, and dissolved in double distilled 5% HNO_3 (Abraham et al., 2008). The dissolved Si was purified by triethylamine molybdate (TEA-moly) co-precipitation and combustion in covered Pt crucibles at 1000 °C (De La Rocha et al., 1996). The combustion product was dissolved in a diluted Suprapur HF-HCl mixture (Cardinal et al., 2003). Silicon isotope compositions were determined using a Nu Plasma

multicollector inductively coupled plasma mass spectrometer (MC-ICP-MS) operating in dry plasma mode, using Mg doping as an external standard to correct mass bias (Cardinal et al., 2003). The isobaric interferences, mostly $^{14}N^{16}O$ on ^{30}Si, were solved following Abraham et al. (2008). Measurements were performed using the sample-standard bracketing technique relative to in-house standards ($pSiO_2$ or Quartz Merck), which are isotopically similar to the quartz reference material NBS28 (National Institute of Standard and Technology RM #8546) (Abraham et al., 2008). The analytical method was validated by an inter-laboratory comparison and the quality of the measurements was controlled by secondary reference materials (diatomite, BHVO-2) along with each samples series, falling on the recommended values (Reynolds et al., 2007; Abraham et al., 2008). Our results were expressed as $\delta^{30}Si$ relative to NBS28 (‰) with an average precision and accuracy on total replicates of ±0.12‰ ($\pm 2\sigma_{SD}$) following:

$$\delta^{30}Si = \left[\frac{\left(\frac{^{30}Si}{^{28}Si}\right)_{sample}}{\left(\frac{^{30}Si}{^{28}Si}\right)_{NBS28}} - 1 \right] \times 1000$$

3. RESULTS

3.1. Soil fractions

The distribution of sand, silt, clay and ASi fractions of the soil layers investigated at the Douglas fir, Black pine and European beech sites is presented in Table 2. The acid brown soil mineral fraction was dominated, in average considering all tree species, by the sand fraction (57.5 ± 1.8 wt%) whereas the fraction of silt (24.5 ± 2.1 wt%) and clay (18.1 ± 2.3 wt%) were less dominant in both 0–7.5 and 30–45 cm layers. The clay-sized fraction in the shallow soil consists of the following minerals: kaolinite (30%) ~ illite (30%) > quartz (20%) > vermiculite (11%) > smectite (4%) > gibbsite (3%) > Fe oxides (2.5%) (Mareschal, 2008). In humus layer (Oh), sand, silt and clay fractions represented, in average considering all tree species, 46.0 ± 8.0%, 48.5 ± 8.0% and 5.6 ± 0.5%, respectively, of the fine earth dry weight of mineral soil incorporated. The proportion of silt was higher in the humus layer (Oh) relative to the mineral soil layer (0–7.5 cm). Through XRD analysis, we identified the following minerals in the clay fraction extracted from humus layer under European beech and Douglas fir: quartz, kaolinite, illite, illite–vermiculite mixed layers, smectite and chlorite. Calvaruso et al. (2009) also detected these clay minerals in the rhizosphere and bulk soil under Norway spruce and oak from the same experimental site. The SiO_2 content of crystallized minerals ranged from 20% (Douglas fir) to 38% (European beech) of humus dry weight and on average 65.2 ± 4.4% in bulk soil dry weight. The ASi content ranged between 0.5% and 1.4% in humus layers, and between 0.3% and 0.6% in bulk soils. The ASi concentrations in humus and soil layers contribute from 3.0% to 7.0% and from 0.4% to 1.0% of the total crystallized SiO_2, respectively.

3.2. Chemical composition of solutions

The chemical compositions of forest floor leachates and soil solutions collected at 60 cm depth under each tree species is presented in Table 3. The pH was generally lower in forest floor leachates than in soil solutions (4.6 ± 0.3 and 5.1 ± 0.3, respectively). The concentrations of DOC, Ca^{2+}, K^{+}, Mg^{2+} and Mn^{2+} were systematically higher in forest floor leachates than in soil solutions. By contrast, the concentrations of Na^{+} and Si were higher in soil solutions than in forest floor leachates.

3.3. Ge/Si ratios

The Ge/Si ratios measured for the five stands are given in Table 4. The Ge/Si ratios of the bedrock, sand and silt fractions were very similar at the European beech site,

Table 2
Distribution (% dry weight in fine earth; <2 mm) of sand, silt, clay and ASi fractions of humus (Oh) and soil layers (0–7.5 and 35–40 cm) under Douglas fir, Black pine, and European beech.

	Sand 50–2000 μm (%)	Silt 2–50 μm (%)	Clay <2 μm (%)	ASi[a] 0–2000 μm (%)	SiO_2[b] 0–2000 μm (%)
Oh					
Douglas fir	43.5	51.5	5.0	1.4	19.7
Black pine	54.9	39.3	5.8	0.5	37.6
European beech	39.5	54.5	6.0	1.2	38.4
Bulk soil 0–7.5 cm					
Douglas fir	57.8	23.0	19.2	0.3	61.7
Black pine	59.2	23.6	17.2	0.5	63.6
European beech	57.6	21.8	20.6	0.6	60.6
Bulk soil 30–45 cm					
Douglas fir	53.9	26.3	19.8	0.4	67.3
Black pine	58.5	27.4	14.1	0.3	72.8
European beech	57.8	24.7	17.5	0.4	65.2

[a] ASi fraction was quantified by alkaline dissolution with Na_2CO_3 solution (Cornelis, 2010).
[b] The SiO_2 content (%) from crystallized minerals corresponds to the total SiO_2 of bulk soil minus the SiO_2 content from ASi (Cornelis et al., 2010).

Table 3
Chemical compositions of forest floor leachates (0 cm) and soil solutions (60 cm) under each tree species.

cm	DOC [a] mg l^{-1}	pH	F^-	Cl^-	SO_4^{2-}	PO_4^{3-}	NO_3^-	Ca^{2+}	K^+	Na^+	Mg^{2+}	Mn^{2+}	S	Fe	Al	Si
			μmol l^{-1}													
Douglas fir																
0	23.5	4.86	1.1	99.3	23.0	8.0	109.0	63.6	44.5	63.1	28.4	14.4	34.9	3.6	20.0	54.8
60	3.7	4.75	4.2	122.1	19.2	0.2	273.4	12.2	21.0	103.1	15.2	6.9	29.0	0.2	53.4	71.9
Norway spruce																
0	53.4	4.62	1.1	92.5	21.0	6.7	46.9	31.4	79.3	57.4	16.5	10.4	36.5	8.8	22.2	53.4
60	3.6	5.18	2.6	137.7	55.1	0	17.1	12.0	25.3	97.9	15.6	4.7	59.9	0.2	13.0	60.9
Black pine																
0	69.0	4.12	1.1	63.8	13.0	0.2	161.4	49.2	109.7	46.1	20.6	18.9	30.3	12.2	64.5	30.6
60	2.4	4.78	3.2	92.8	50.7	0	82.6	12.0	13.0	75.3	9.5	6.0	53.3	0.2	31.9	80.8
European beech																
0	32.5	4.41	0.5	36.1	11.6	1.2	49.7	29.4	41.2	23.9	9.5	11.6	20.3	7.7	27.4	34.5
60	2.3	5.52	2.1	57.8	38.8	0.2	1.9	3.5	8.7	58.7	6.2	3.3	42.1	0.2	7.8	60.2
Oak																
0	37.0	5.05	0.5	42.0	15.0	5.4	69.7	36.9	39.1	32.2	18.1	10.9	25.9	5.7	39.7	64.5
60	2.6	5.19	1.6	33.3	52.3	0.3	7.6	6.2	4.9	39.1	7.4	1.8	53.3	0.2	10.4	67.0

[a] DOC, dissolved organic carbon.

ranging from 2.3 to 2.5 μmol mol^{-1}. In contrast, the clay fraction displayed the highest Ge/Si ratio (6.2 ± 0.08 μmol mol^{-1}, $n = 2$, $\pm 1\sigma$SD, two repetitions on two different depths) at this site. The Ge/Si ratios of bulk soils were similar under each tree species, at 2.5 ± 0.1 and 2.6 ± 0.2 μmol mol^{-1} ($n = 5$, $\pm 1\sigma$SD) for 0–7.5 and 30–45 cm bulk soil, respectively. Therefore, we assume that the Ge/Si ratios of sand, silt and clay fractions measured under European beech are also representative for the other sites investigated. The Ge/Si ratios measured in leaves/needles were similar for each species, ranging from 0.1 to 0.3 μmol mol^{-1}, except of pine needles with a Ge/Si ratio of 1.5 μmol mol^{-1}. In organic horizons (Of and Oh), Ge/Si ratios were higher than in leaves/needles with 2.7 ± 0.9 μmol mol^{-1} ($n = 5$, $\pm 1\sigma$SD) in Of and 3.2 ± 0.2 μmol mol^{-1} ($n = 5$, $\pm 1\sigma$SD) in Oh. At each investigated site, the Si concentrations were lower in forest floor leachates than in soil solutions while the forest floor leachates were more enriched in Ge compared to soil solutions. Consequently, Ge/Si ratios were higher in forest floor leachates than in soil solutions collected. More particularly, forest floor leachates under Black pine, European beech and oak displayed higher Ge/Si ratios (2.3–3.7 μmol mol^{-1}) relative to Douglas fir and Norway spruce (1.6–2.1 μmol mol^{-1}). In soil solutions, Ge/Si ratios were similar under each tree species (1.2 ± 0.2 μmol mol^{-1}, $n = 5$, $\pm 1\sigma$SD).

3.4. Si-isotopic compositions

The Si-isotopic signatures under Douglas fir and European beech stands are given in Table 5 ($\pm 1\sigma$SD on replicates n; Table 5). The sand fraction at the European beech site, mainly containing primary minerals, displayed a δ^{30}Si value of -0.03 ± 0.07‰, which is close to that of granitic bedrock (-0.07 ± 0.03‰). Silt and clay fractions were significantly isotopically lighter than granitic bedrock, with δ^{30}Si values of -0.60 ± 0.28‰ and -1.07 ± 0.32‰, respectively. Bulk soils sampled at 0–7.5 cm and 30–45 cm displayed δ^{30}Si values of -0.06 ± 0.12‰ and $+0.08 \pm 0.07$‰, respectively, which is similar to the signature of the granitic bedrock.

The δ^{30}Si values of the BSi and the humus layer (Oh) at European beech stand were significantly isotopically lighter (-0.64 ± 0.02‰ and -0.68 ± 0.04‰, respectively) than in Douglas fir stand (-0.28 ± 0.11‰ and -0.34 ± 0.08‰, respectively).

The DSi of the forest floor leachates were depleted in heavy Si isotopes compared to the bedrock showing δ^{30}Si values of -1.38 ± 0.17‰ at the Douglas fir site and -2.05 ± 0.12‰ at the European beech site, respectively.

4. DISCUSSION

4.1. δ^{30}Si and Ge/Si ratios in solid samples

As illustrated in Fig. 1, unweathered granitic bedrock displays δ^{30}Si signature of -0.07‰, which is in agreement with values previously reported for granitic rocks (average δ^{30}Si value $= -0.07 \pm 0.05$‰ ($\pm 2\sigma_{SEM}$, $n = 47$; see overview of André et al., 2006)). The Si isotopic and Ge/Si signatures of the bedrock are close to those of granitoid rocks at Luquillo (Puerto Rico) (δ^{30}Si $= -0.2$‰, Ziegler et al., 2005b; Ge/Si $= 2.0$–2.4 μmol mol^{-1}, Kurtz et al., 2002; Lugolobi et al., 2010). Clay mineral neoformation produces lighter δ^{30}Si values in secondary clay minerals relative to the bedrock (Ziegler et al., 2005a,b). With increasing soil weathering degree, clay fractions were shown to be increasingly enriched in light Si isotopes (Ziegler et al., 2005b; Opfergelt et al., 2008, 2010) with values of -2.2 ± 0.2‰ for kaolinite in the tropical granitic weathering environment at Luquillo (Ziegler et al., 2005b). In this latter tropical environment, clay minerals were thus ~2.0‰ more negative than the granitic parent material. This difference is larger than in our temperate ecosystem where the clay

Table 4
Si and Ge concentrations and Ge/Si ratios in the compartments of the soil–tree system under five forest stands: bedrock; bulk soils at 0–7.5 and 30–45 cm (<2000 μm); sand (>50 μm), silt (2–50 μm), and clay (<2 μm) fractions; leaves and needles; fragmented organic horizon (Of), humified organic horizon (Oh); forest floor leachates, and soil solution collected at 60 cm depth.

	Si (mmol g^{-1})	Ge (nmol g^{-1})	Ge/Si (μmol mol^{-1})
Bedrock	12.6	32.1	2.5
Sand[a]	13.1	29.5	2.3
Silt	12.1	30.4	2.5
Clay 1[b]	8.51	53.3	6.3
Clay 2	8.30	51.0	6.1
Douglas fir			
Needles	0.21	0.04	0.2
Of	0.83	1.71	2.0
Oh	3.53	11.85	3.4
Forest floor leachate	0.08	0.158	2.1
Bulk soil 0–7.5	11.13	27.92	2.5
Bulk soil 30–45	11.54	31.97	2.8
Soil solution	0.09	0.11	1.3
Norway spruce			
Needles	0.32	0.03	0.1
Of	0.73	1.06	1.4
Oh	1.72	5.10	3.0
Forest floor leachate	0.05	0.08	1.6
Bulk soil 0–7.5	10.95	26.90	2.5
Bulk soil 30–45	11.76	29.21	2.5
Soil solution	0.07	0.07	1.0
Black pine			
Needles	0.01	0.02	1.5
Of	1.72	6.02	3.5
Oh	5.68	17.67	3.1
Forest floor leachate	0.04	0.16	3.7
Bulk soil 0–7.5	10.83	28.17	2.6
Bulk soil 30–45	11.68	31.53	2.7
Soil solution	0.10	0.12	1.2
European beech			
Leaves	0.25	0.05	0.2
Of	2.20	7.55	3.4
Oh	6.03	21.24	3.5
Forest floor leachate	0.043	0.101	2.3
Bulk soil 0–7.5	11.39	26.23	2.3
Bulk soil 30–45	11.81	28.00	2.4
Soil solution	0.067	0.095	1.4
Oak			
Leaves	0.17	0.05	0.3
Of	1.09	3.65	3.4
Oh	6.82	20.73	3.0
Forest floor leachate	0.037	0.165	3.7
Bulk soil 0–7.5	11.09	29.52	2.7
Bulk soil 30–45	11.55	29.55	2.6
Soil solution	0.086	0.094	1.1

[a] Sand, silt and clay fractions were separated from soil collected under European beech.
[b] Clay 1 = clay-sized minerals from the humus layer (Oh) at European beech site; Clay 2 = clay-sized minerals from the 30–45 cm mineral layer at European beech site.

Table 5
Si-isotopic signatures (δ^{30}Si $\pm 1\sigma_{SD}$; ‰) of (1) bedrock, soil between 0–7.5 cm and 30–45 cm depth (<2000 μm), sand (>50 μm), silt (2–50 μm) and clay (<2 μm) fractions collected under European beech stand, and (2) biogenic Si (BSi), humus layer (Oh) and forest floor leachates collected under European beech and Douglas fir stands.

	n[a]	δ^{30}Si (‰)	$1\sigma_{SD}$
Bedrock	2	−0.07	0.03
Sand	3	−0.03	0.07
Silt	4	−0.60	0.28
Clay	4	−1.07	0.32
Bulk soil 0–7.5 cm	2	−0.06	0.12
Bulk soil 30–45 cm	2	+0.08	0.07
Douglas fir			
BSi	2	−0.28	0.11
Oh	2	−0.34	0.08
Forest floor leachate	4	−1.38	0.17
European Beech			
BSi	2	−0.64	0.02
Oh	3	−0.68	0.04
Forest floor leachate	1	−2.05	0.12[b]

[a] n = measurement replicates.
[b] $2\sigma_{SEM}$ = internal error of the measurement.

fraction displays a δ^{30}Si value 1.0‰ lighter than the granitic bedrock. This difference can be explained by a distinct clay mineralogy mainly composed of kaolinite in the tropical environment (Ziegler et al., 2005b) and of kaolinite and other clay minerals such as illite, vermiculite, and smectite in the present study. Indeed, the clay fraction in Puerto Rico derives from parental granite with a slightly different mineralogy (25% quartz, 56% plagioclase, 10% biotite; Ziegler et al., 2005b) than the granite at our site (34.5% quartz, 24% feldspars, 30.7% albite, 8.5% muscovite, 1.7% biotite and 0.6% chlorite; Ranger et al., 2004; Mareschal, 2008). High Ge/Si ratios in our clay fractions (6.2 ± 0.08 μmol mol^{-1}), close to that of kaolinite at Luquillo ranging between 4.8 and 6.1 μmol mol^{-1} (Lugolobi et al., 2010), are due to incongruent weathering reactions leading to an enrichment of Ge in secondary clay minerals relative to primary minerals (Kurtz et al., 2002; Opfergelt et al., 2010).

Si uptake by plants produces lighter δ^{30}Si values in BSi relative to source solution (Ding et al., 2005; Opfergelt et al., 2006a). In trees, the Si-isotopic signatures of BSi from Douglas fir (−0.28‰) and European beech (−0.64‰) are negative, a feature which has also been observed on Downy birch (−0.22‰) from boreal forest (Engström et al., 2008). Since the root biomass is mostly distributed between 0 and 70 cm depth (Ranger et al., 2004), the DSi source for tree uptake is not limited to the DSi from the forest floor leachates, reported to be isotopically lighter than BSi. Except for pine (1.5 μmol mol^{-1}), leaves and needles display low Ge/Si ratios (0.1–0.3 μmol mol^{-1}) as reported by Blecker et al. (2007) and Delvigne et al. (2009). The latter authors suggest that Ge is organically trapped in roots.

In our study, the humus layers (Oh) display high Ge/Si ratios. This enrichment in Ge suggests two different processes: (1) an accumulation of secondary clay minerals due to bioturbation (Cornelis et al., 2010), and/or (2) the formation of organic complexes between Ge and carboxylic

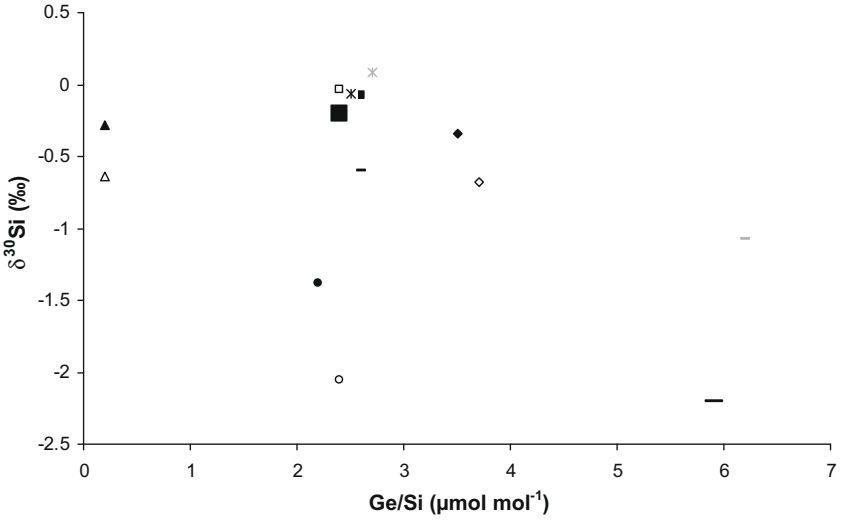

Fig. 1. δ^{30}Si values plotted versus Ge/Si ratios in bedrock (black square); sand (open square), silt (black dash) and clay (grey dash) fractions, 0–7.5 cm bulk soil (black star) and 30–45 cm bulk soil (grey star) under European beech; BSi (triangles), humus layer (diamonds), and forest floor leachates (circles) under European beech (open) and Douglas fir (black). For comparison: Granite = large black square (δ^{30}Si: Ziegler et al., 2005b; Ge/Si: Kurtz et al., 2002; Lugolobi et al., 2010), Kaolinite from granitic parent material = large black dash (δ^{30}Si: Ziegler et al., 2005b; Ge/Si: Kurtz et al., 2002).

functional groups of the humic acids in the organic-rich horizons (Pokrovski et al., 2000). Considering δ^{30}Si values and Ge/Si ratios of all soil fractions and the proportion of Si in each fraction (sand, silt, clay and ASi fractions) in humus layer of the Douglas fir site, a bulk Si-isotopic and Ge/Si signature of humus layer (Oh) can be calculated by mass balance equation (Opfergelt et al., 2010) (Table 6). The calculated δ^{30}Si value of Douglas fir humus layer (-0.43 ± 0.17‰) does not differ significantly from measured δ^{30}Si value (-0.34 ± 0.08‰). This is confirmed by the Ge/Si mass balance: the calculated Ge/Si ratio of Douglas fir Oh (3.1 µmol mol^{-1}) does not differ from measured Ge/Si (3.4 µmol mol^{-1}). This suggests that all the Si pools have been identified and that the δ^{30}Si values and Ge/Si ratio in the Oh under Douglas fir are governed by the proportion of biogenic, primary and secondary clay minerals. A similar calculation can be done for the bulk soil at 0–7.5 cm depth of the Douglas fir site. The calculated δ^{30}Si value (-0.32 ± 0.17‰) is not significantly different from measured δ^{30}Si value (-0.06 ± 0.12‰), which confirms that all Si pools have been identified. In addition, the calculated Ge/Si ratio (2.3 µmol mol^{-1}) does not differ from measured Ge/Si (2.5 µmol mol^{-1}) for the bulk soil at 0–7.5 cm depth of the Douglas fir site.

Cornelis et al. (2010) demonstrate that the content of litho/pedogenic minerals in the Oh is strongly influenced by bioturbation rates. Indeed, following bioturbation indexes, the incorporation of soil minerals into organic horizons is less important under Douglas fir and Norway spruce than under Black pine, European beech and oak. This was supported by lower concentration of SiO_2 inherited from soil minerals in Oh under Norway spruce (11.6%) and Douglas fir (20.4%), in comparison with Black pine (37.9%), European beech (39.3%) and oak (43.6%) (Cornelis et al., 2010). In the present study, Ge/Si ratios in Of are lower under Douglas fir and Norway spruce (2.0 and 1.4 µmol mol^{-1}, respectively) than under Black pine, European beech and oak (3.4 ± 0.06 µmol mol^{-1}, $n = 3$, 1σSD). These results suggest that the incorporation of clay-sized minerals (characterized by relatively higher Ge/Si ratios) in organic horizons is more important under Black pine, European beech and oak than under Douglas fir and Norway spruce, driving the lower Ge/Si ratio in the latter group. This is in good agreement with the findings of Cornelis et al. (2010) based on bioturbation.

4.2. δ^{30}Si and Ge/Si ratios variations in solutions

The δ^{30}Si values in forest floor leachates collected under Douglas fir and European beech (-1.38‰ and -2.05‰, respectively) are more negative than the isotopically lightest natural waters reported by Georg et al. (2009). The forest floor leachates are isotopically lighter than clay fraction (-1.07‰) and than BSi (ranging from -0.28 to -0.64‰). For all tree species, the forest floor leachate solutions display higher Ge/Si ratios than soil solutions (Table 4). These findings contrast with soil solutions from Hawaii shown to display heavier Si-isotopic signatures relatively to secondary precipitates preferentially incorporating light Si isotopes (Ziegler et al., 2005a).

Our soil solutions display similar Ge/Si ratios for all tree species (1.2 ± 0.2 µmol mol^{-1}) suggesting a pedogenic control on DSi (weathering of primary minerals, neoformation of secondary clay minerals and Si adsorption onto Al and Fe (hydr)oxides). Moreover, soil solutions have lower Ge/Si ratios than the bedrock revealing the impact of secondary clay minerals neoformation on the Ge depletion (Kurtz et al., 2002).

To further investigate the origin of these forest floor leachates signatures, the ion concentration of solutions (Table 3) was used to calculate the saturation index (PHREEQC Version 2; Parkhurst and Appelo, 1999) with

Table 6
Si-isotopic and Ge/Si mass balance calculation to evaluate the bulk Si-isotopic and Ge/Si signatures of Oh and bulk soil at 0–7.5 cm depth under Douglas fir, from all the solid Si pools (% dry weight of humus and fraction <2 mm, respectively).

	Sand fraction			Silt fraction			Clay fraction			ASi fraction						
	%[a]	SiO_2[b]%	Proportion[c]	%[a]	SiO_2[b]%	Proportion[c]	%[a]	SiO_2[b]%	Proportion[c]	%[a]	SiO_2[b]%	Proportion[c]	$\delta^{30}Si$ calculated[d]	$\delta^{30}Si$ measured	Ge/Si calculated	Ge/Si measured
Oh	14.3	80.3	0.54	16.6	76.8	0.60	1.8	47.1	0.04	0.4	98	0.02	−0.43 (0.17)	−0.34 (0.08)	3.1	3.4
0–7.5 (cm)	57.8	80.3	0.68	23.0	76.8	0.26	19.2	47.1	0.13	0.3	98	0.004	−0.32 (0.17)	−0.06 (0.12)	2.3	2.5

[a] Sand, silt, clay and ASi contents.
[b] SiO_2 content in fractions.
[c] SiO_2 proportion in sand, silt, clay and ASi fractions calculated as follows [(% fraction × SiO_2% in fraction)/SiO_2% in bulk]/100. The SiO_2 concentration in bulk Oh and 0–7.5 cm soil layer, are respectively, 21.2% and 68.4%.
[d] The contribution of each fractions to the Si-isotopic and Ge/Si bulk soil signature can be calculated by multiplying the $\delta^{30}Si$ or Ge/Si signature of each fraction (from data in Tables 4 and 5) by the proportion of SiO_2 of each fraction ([c] in this table). The bulk soil signature represents the sum of the contribution of each fraction. The standard deviation ($\pm 1\sigma_{SD}$) is calculated by the method of the propagation of uncertainty.

respect to minerals incorporated in the organic horizons by bioturbation. Saturation index calculations show that forest floor leachates are undersaturated with respect to albite, anorthite, chlorites, illite, Ca-montmorillonite, K-feldspar, quartz and amorphous silica and are oversaturated with K-mica and kaolinite (Fig. 2). Without considering the fact that organic acids promote dissolution of minerals, this simple mineral stability calculation show that clay minerals detected by XRD in the humus layer such as vermiculite, chlorite, illite, and Ca-montmorillonite (smectite) are not stable and could be partially dissolved and transformed in the chemical environment of forest floor. Thus, low pH (4.6 ± 0.3) and high concentration of low molecular organic acids in the organic horizons ($DOC = 43.1 \pm 18.1$ mg l^{-1}) relative to mineral soil ($DOC = 2.9 \pm 0.7$ mg l^{-1}) make it very likely that clay minerals dissolve (Giesler et al., 2000). Indeed clay dissolution favored by the action of organic acids has already been recognized to explain high dissolved element contents in tropical organic-rich rivers (Gaillardet et al., 1995) or soil solutions (Oliva et al., 1999). Barman et al. (1992) also conclude that organic acids dissolve minerals through acid attack and complexation. In organic environment, the hydroxyl inter-layered 2:1 clay minerals lose their Al-interlayers and transform into vermiculite and smectite, which in turn weather, producing large amount of Mg in the solution (Brahy et al., 2000). This process is confirmed in our study by the identification of smectite in the clay fraction from the humus layer and the high content of Mg^{2+} in forest floor leachates relative to soil solution (Table 3), which support weathering of Mg-bearing phyllosilicates in humus layers.

The $\delta^{30}Si$ and Ge/Si data presented above are useful to infer the relative roles of biogenic and inorganic minerals on the release of DSi in forest floor leachate solutions. Indeed, the Si-isotopic composition and Ge/Si ratios of forest floor leachates can be impacted by both biological processes (recycling of biogenic silica in the shallow soil) and by pedogenic processes (weathering of primary minerals and formation/dissolution of secondary clay minerals incorporated in organic horizons by bioturbation). The present study highlights that DSi is controlled by clay dissolution rather than BSi recycling, as supported by Si-isotopically light and Ge-enriched forest floor leachates. In this granitic environment, the stock of ASi, including BSi fraction, seems too low in comparison with the stock of crystallized minerals to significantly influence the DSi release in forest floor leachate and in soil solutions. The Si-isotopic signature and Ge/Si ratio of DSi in the forest floor leachates would represent a bulk signature of the dissolution of sand, silt, clay and ASi fractions (Opfergelt et al., 2010). In our case, the measured Si-isotopic signature of forest floor leachates (−1.38‰ and −2.05‰) cannot be explained by a congruent dissolution of primary and secondary minerals with an additional contribution from ASi, since the forest floor leachates are isotopically lighter than all components. Moreover, Ge/Si ratios of clay fractions are too high to explain the Ge/Si ratios in the forest floor leachates by congruent dissolution of clay minerals. The ^{28}Si enrichment in forest floor leachates could be explained by the preferential release of light Si isotopes during partial dissolution of

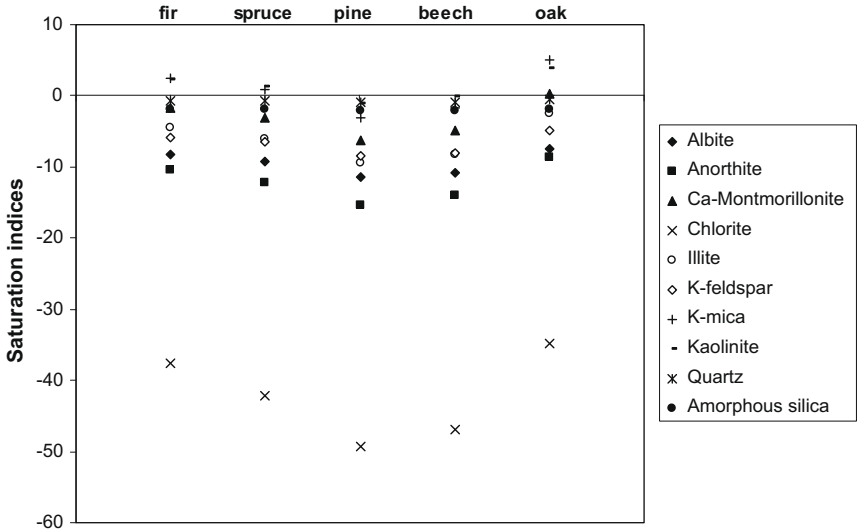

Fig. 2. Calculated saturation indices (PHREEQC-2) in forest floor leachates for primary and secondary minerals admixed in humus layer (Oh) by bioturbation, as revealed by XRD analysis under the five tree species: Douglas fir, Norway spruce, Black pine, European beech, and oak.

clay minerals as seen for BSi (Demarest et al., 2009) and volcanic glass (Ziegler et al., 2005a). Dissolution of clay and silt admixed in the humus layer (Oh) would, therefore, also release Ge, which could be temporarily organically trapped with organic matter (Delvigne et al., 2009). A release of Ge from clay minerals and Ge-organically trapped could explain high Ge/Si ratio in forest floor leachates.

Based on (1) the contrast between Ge/Si ratios and Si-isotopic compositions, (2) the important stock of soil minerals in humus layer relative to the BSi stock, and (3) the chemical conditions in organic horizons, it seems reasonable to assume that the partial dissolution of clay minerals greatly influences the source of DSi in forest floor leachates.

These combined data suggest that the enrichment in ^{28}Si and Ge in forest floor leachates could be twofold. It could reflect a preferential release of a light Si isotopes and Ge during clay dissolution. Besides, Si adsorbed onto Fe-oxides (2.5% of the clay fraction; Mareschal, 2008) known to be enriched in light Si isotopes (Delstanche et al., 2009; Opfergelt et al., 2009) could be released by desorption. This could explain low $\delta^{30}Si$ values of DSi in forest floor leachates.

4.3. Implications on biogeochemical Si cycle in forest ecosystem

The Si isotope and Ge/Si signatures in forest soil solutions likely reflect a complex interaction of (i) primary, secondary and biogenic mineral dissolution and mineral transformation, (ii) uptake by forest vegetation, (iii) Si adsorption onto secondary phases, and (iv) Si export from the soil profile. DSi content in forest floor leachates is tree species-dependent mainly through various incorporation of soil minerals in organic horizons by bioturbation (Cornelis et al., 2010) and only secondarily through the recycling of BSi on topsoil (Table 7). Indeed, Ge/Si ratio in forest floor leachates can be related to Si recycling rate and bioturbation estimated under each tree species (Cornelis et al., 2010). The Ge/Si ratio in forest floor leachates decreases following the sequence Black pine $\geqslant$ oak $>$ European beech $>$ Douglas fir $>$ Norway spruce (3.7, 3.7, 2.3, 2.1 and 1.6 μmol mol^{-1}, respectively; Table 4). This can be related to a higher bioturbation in Black pine, oak, European beech than in Douglas fir and Norway spruce (Cornelis et al., 2010), claiming for a decreasing impact of clay dissolution on the DSi from Black pine to Norway spruce. In parallel, recycling of Si increases following the sequence Black pine $<$ oak $<$ European beech $<$ Douglas fir $<$ Norway spruce (2.3, 18.5, 23.3, 30.6 and 43.5 kg ha^{-1} yr^{-1}, respectively; Table 7). This supports an increasing impact of BSi dissolution from Black pine to Norway spruce (since BSi is depleted in Ge) supporting the lower Ge/Si ratio in forest floor leachate under Norway spruce. $\delta^{30}Si$ values in forest floor leachates also support a larger influence of partial clay mineral dissolution in humus layer under European beech than under Douglas fir, as the lighter Si-isotopic

Table 7
Mean values of Si uptake and Si restitution on topsoil through litterfall in five common tree species studied in same climatic and soil conditions (Cornelis et al., 2010).

	Si (kg ha^{-1} yr^{-1})				
	Douglas fir	Norway spruce	Black pine	European beech	Oak
Uptake	30.6	43.5	2.3	23.3	18.5
Litterfall	29.0	42.2	2.1	19.3	17.8

signature is under European beech. Besides, even if the Si recycling suggests a higher impact of BSi dissolution under Douglas fir than under European beech, δ^{30}Si of BSi is lighter under European beech (−0.64‰) compared to Douglas fir (−0.28‰). Dissolution of BSi would, therefore, potentially provide a lighter Si source for DSi in forest floor leachate under European beech.

5. CONCLUSIONS

This study traced the sources and mechanisms controlling the release of DSi in forest floor leachates and soil solutions using stable Si isotopes and the Ge/Si ratio in well defined soil–tree systems in a temperate granitic environment.

Our results show that Si-isotopic signatures and Ge/Si ratios of forest floor leachates evolve towards lighter δ^{30}Si values (−1.38‰ and −2.05‰) and higher Ge/Si ratios (2.7 ± 1.0 μmol mol^{-1}, $n = 5$, 1σSD), relative to granite bedrock. Sources of dissolved Si in forest floor leachates are influenced by tree species, which determine the extent of mixing of clay minerals in organic horizons by bioturbation while the source of DSi in soil solution is essentially impacted by pedogenic processes. This suggests a difference in the soil mineral weathering regime relative to depth and soil chemistry conditions: more secondary mineral weathering in organic horizons and greater stability of secondary minerals in deeper soil layers.

Although tree species take up to 43.5 kg Si ha^{-1} yr^{-1}, which constitutes a large amount of BSi restituted on topsoil (Cornelis et al., 2010), dissolution of phytoliths does not seem to control the DSi composition of the forest floor leachates, even given the high reported dissolution rates for phytoliths (Fraysse et al., 2009). Indeed, the ASi stock, including BSi, in organic horizon is low relative to crystallized Si stock. Our results are consistent with the observations in a tropical granitic catchment (Ziegler et al., 2005b; Lugolobi et al., 2010), but stand in marked contrast either the results of Derry et al. (2005) showing a strong biological control on Si cycling and export in basaltic soils with very low availability of mineral-derived Si.

In order to better assess the relative contributions from biogenic and litho/pedogenic sources to soil solutions, it would be interesting to study the seasonal variations of Si-isotopic signature and Ge/Si ratios in forest floor leachates and soil solutions.

ACKNOWLEDGMENTS

We thank D. Gelhaye (INRA) and A. Lannoye (UCL) for field assistance, N. Mattielli and J. de Jong (ULB) for managing the MC-ICP-MS facility in ULB, and A. Iserentant and C. Givron (UCL), J. Navez, L. Monin and N. Dahkani (RMCA) for laboratory assistance. We also thank Camille Delvigne (RMCA), Sophie Chassery (Ut2a-Pau) and Delphine Yeghicheyan (SARM-CRPG) for the analyses of the Ge and Si. The manuscript has greatly benefited from the constructive comments of G. Steinhoefel and of two anonymous referees. J.-T. Cornelis is supported by the « Fonds pour la formation à la Recherche dans l'Industrie et dans l'Agriculture » (FRIA) of Belgium, S.O. by the « Fonds National de la Recherche Scientifique » (FNRS) of Belgium, and D.C. by the Federal Belgian Science Policy (BELSPO, IAP P6/13). The Breuil-Chenue site belongs to the ORE network (long term observation of forest ecosystems) and received funds from the GIP ECOFOR for monitoring. This research was supported by the "Fonds Spécial de Recherche" (FSR) 2008 of the UCL. The Si isotopes methodology has been set up owing to various supports from BELSPO (EV/37/7C, IAP P6/13), FNRS (FRFC 2.4.512.00F), the EC (EVK-CT-2000-00057).

REFERENCES

Abraham K., Opfergelt S., Fripiat F., Cavagna A.-J., de Jong J. T. M., Foley S., André L. and Cardinal D. (2008) δ^{30}Si and δ^{29}Si determinations on BHVO-1 and BHVO-2 reference materials via new configuration on Nu Plasma Multi Collector (MC)-ICP-MS. *Geostand. Geoanal. Res.* **32**, 193–202.

Alexandre A., Meunier J.-D., Colin F. and Koud J. M. (1997) Plant impact on the biogeochemical cycle of silicon and related weathering processes. *Geochim. Cosmochim. Acta* **61**, 677–682.

Alleman L. Y., Cardinal D., Cocquyt C., Plisnier P. D., Descy J. P., Kimirei I., Sinyinza D. and André L. (2005) Silicon isotopic fractionation in lake Tanganyika and its main tributaries. *J. Great Lakes Res.* **31**, 509–519.

André L., Cardinal D., Alleman L. Y. and Moorbath S. (2006) Silicon isotopes in 3.8 Ga West Greenland rocks as clues to the Eoarchean supracrustal Si cycle. *Earth Planet. Sci. Lett.* **245**, 162–173.

Aurousseau P. (1976) Morphologie et genèse des sols sur granite du Morvan. Ph. D. thesis, Université de Rennes, 210 p.

Azam F. and Volcani B. E. (1981) Germanium–silicon interactions in biological systems. In *Silicon and Siliceous Structures in Biological Systems* (eds. T. L. Simpson and B. E. Volcani). Springer-Verlag, New York, pp. 43–67.

Barman A. K., Varadachari C. and Ghosh K. (1992) Weathering of silicate minerals by organic acids. I. Nature of cation solubilisation. *Geoderma* **53**, 45–63.

Bartoli F. (1983) The biogeochemical cycle of silicon in two temperate forest ecosystems. *Environ. Biogeochem. Ecol. Bull.* **35**, 469–476.

Basile-Doelsch I. (2006) Si stable isotopes in the Earth's surface: a review. *J. Geochem. Explor.* **88**(1–3), 252–256.

Berner R. A. (1997) The rise of plants and their effect on weathering and atmospheric CO_2. *Science* **276**, 544.

Blecker S. W., King S. L., Derry L. A., Chadwick O. A., Ippolito J. A. and Kelly E. F. (2007) The ratio of germanium to silicon in plant phytoliths: Quantification of biological discrimination under controlled experimental conditions. *Biogeochemistry* **86**, 189–199.

Bonneau M., Brêthes A., Lacaze J. F., Lelong F., Levy G., Nys C. and Souchier B. (1977) Modification de la fertilité des sols sous boisement artificiel de résineux purs. C.R. Fin d'Etude D.G.R.S.T., Nancy-Champenoux, p. 88.

Brahy V., Titeux H. and Delvaux B. (2000) Incipient podzolization and weathering caused by complexation in a forest Cambisol on loess as revealed by a soil solution study. *Eur. J. Soil. Sci.* **51**, 475–484.

Calvaruso C., Mareschal L., Turpault M.-P. and Leclerc E. (2009) Rapid clay weathering in the rhizosphere of Norway spruce and oak in an acid forest ecosystem. *Soil Sci. Soc. Am. J.* **73**, 331–338.

Cardinal D., Alleman L. Y., De Jong J., Ziegler K. and André L. (2003) Isotopic composition of silicon measured by multicollector plasma source mass spectrometry in dry plasma mode. *J. Anal. Atom. Spectrom.* **18**, 213–218.

Carignan J., Hild P., Mevelle G., Morel J. and Yeghicheyan D. (2001) Routine analyzes of trace element in geological samples using flow injection and low pressure on-line liquid chromatography coupled to ICP-MS: a study of geochemical reference materials BR, DR-N, UB-N, AN-G and GH. *Geostand. Newsl.* **25**, 187–198.

Conley D. J. (2002) Terrestrial ecosystems and the global biogeochemical silica cycle. *Global Biogeochem. Cycles* **16**(4), 1121.

Cornelis J.-T., Ranger J., Iserentant A. and Delvaux B. (2010) Tree species impact the terrestrial cycle of silicon through various uptakes. *Biogeochemistry* **97**, 231–245.

Cornelis J.-T. (2010) Impact of tree species on silicon cycling in temperate soil-tree systems. Ph.D. thesis, Université catholique de Louvain, Louvain-la-Neuve, p. 223.

De La Rocha C. L., Brzezinski M. A. and De Niro M. J. (1996) Purification, recovery, and laser-driven fluorination of silicon dissolved and particulate silica for the measurement of natural stable isotope abundances. *Anal. Chem.* **68**, 3746–3750.

De La Rocha C. L., Brzezinski M. A. and De Niro M. J. (2000) A first look at the distribution of the stable isotopes of silicon in natural waters. *Geochim. Cosmochim. Acta* **64**, 2467–2477.

Delstanche S., Opfergelt S., Cardinal D., Elsass F., André L. and Delvaux B. (2009) Silicon isotopic fractionation during adsorption of aqueous monosilicic acid onto iron oxide. *Geochim. Cosmochim. Acta* **73**, 923–934.

Delvigne C., Opfergelt S., Cardinal D., Delvaux B. and André L. (2009) Distinct silicon and germanium pathways in the soil–plant system: evidence from banana and horsetail. *J. Geophys. Res. Biogeosciences* **114**, G02013, doi:10.1029/2008JG000899.

Demarest M. S., Brzezinski M. A. and Beucher C. P. (2009) Fractionation of silicon isotopes during biogenic silica dissolution. *Geochim. Cosmochim. Acta* **73**, 5572–5583.

Derry L. A., Kurtz A. C., Ziegler K. and Chadwick O. A. (2005) Biological control of terrestrial silica cycling and export fluxes to watersheds. *Nature* **433**, 728–731.

Ding T., Wan D., Wang C. and Zhang F. (2004) Silicon isotope compositions of dissolved silicon and suspended matter in the Yangtze River, China. *Geochim. Cosmochim. Acta* **68**, 205–216.

Ding T. P., Ma G. R., Shui M. X., Wan D. F. and Li R. H. (2005) Silicon isotope study on rice plants from the Zhejiang province, China. *Chem. Geol.* **218**, 41–50.

Ding T. P., Zhou J. X., Wan D. F., Chen Z. Y., Wang C. Y. and Zhang F. (2008) Silicon isotope fractionation in bamboo and its significance to the biogeochemical cycle of silicon. *Geochim. Cosmochim. Acta* **72**, 1381–1395.

Douthitt C. B. (1982) The geochemistry of the stable isotopes of silicon. *Geochim. Cosmochim. Acta* **46**, 1449–1458.

Engström E., Rodushkin I., Öhlander B., Ingri J. and Baxter D. C. (2008) Silicon isotopic composition of boreal forest vegetation in Northern Sweden. *Chem. Geol.* **247**, 247–256.

Fraysse F., Pokrovsky O. S., Schott J. and Meunier J. D. (2009) Surface chemistry and reactivity of plant phytoliths in aqueous solutions. *Chem. Geol.* **258**, 197–206.

Gaillardet J., Dupre B. and Allegre C. J. (1995) A global geochemical mass budget applied to the Congo Basin rivers: Erosion rates and continental crust composition. *Geochim. Cosmochim. Acta* **59**, 3469–3485.

Gaillardet J., Dupre B. and Allegre C. J. (1999) Geochemistry of large river suspended sediments: Silicate weathering or recycling tracer? *Geochim. Cosmochim. Acta* **63**(23–24), 4307–4351.

Georg R. B., Reynolds B. C., Frank M. and Halliday A. N. (2006) Mechanisms controlling the silicon isotopic compositions of river waters. *Earth Planet. Sci. Lett.* **249**, 290–306.

Georg R. B., Reynolds B. C., West A. J., Burton K. W. and Halliday A. N. (2007) Silicon isotope variations accompanying basalt weathering in Iceland. *Earth Planet. Sci. Lett.* **261**, 476–490.

Georg R. B., Zhu C., Reynolds B. C. and Halliday A. N. (2009) Stable silicon isotopes of groundwater, feldspars, and clay coatings in the Navajo Sandstone aquifer, Black Mesa, Arizona, USA. *Geochim. Cosmochim. Acta* **73**, 2229–2241.

Giesler R., Ilvesniemi H., Nyberg L., van Hees P., Starr M., Bishop K., Kareinen T. and Lundström U. S. (2000) Distribution and mobilization of Al, Fe and Si in three podzolic soil profiles in relation to the humus layer. *Geoderma* **94**, 149–263.

Henriet C., De Jaeger N., Dorel M., Opfergelt S. and Delvaux B. (2008) The reserve of weatherable primary silicates impacts the accumulation of biogenic silicon in volcanic ash soils. *Biogeochemistry* **90**, 209–223.

Hodson M. J., White P. J., Mead A. and Broadley M. R. (2005) Phylogenetic variation in the silicon composition of plants. *Ann. Bot.* **96**, 1027–1046.

IUSS Working Group WRB (2006) World reference base for soil resources 2006, 2nd ed. World Soil Resources Reports No. 103. FAO, Rome.

Jones L. H. P. and Handreck K. A. (1965) Studies of silica in the oat plant. III. Uptake of silica from soils by plant. *Plant Soil* **23**(1), 79–96.

Kelly E. F., Chadwick O. A. and Hilinski T. E. (1998) The effect of plants on mineral weathering. *Biogeochemistry* **42**, 21–53.

Kurtz A. C. and Derry L. A. (2004) Tracing silicate weathering and terrestrial silica cycling with Ge/Si ratios. In *Proceedings of 11th International Symposium on Water Rock Interaction* (eds. R. B. Wanty and R. R. Seal). A.A. Balkema, Leiden, Netherlands, pp. 833–836.

Kurtz A., Derry L. A. and Chadwick O. A. (2002) Germanium–silicon fractionation in the weathering environment. *Geochim. Cosmochim. Acta* **66**, 1525–1537.

Lucas Y. (2001) The role of plants in controlling rates and products of weathering: importance of biological pumping. *Annu. Rev. Earth Planet. Sci.* **29**, 135–163.

Lucas Y., Luizao F. J., Chauvel A., Rouiller J. and Nahon D. (1993) The relation between biological activity of the rain forest and mineral composition of soils. *Science* **260**, 521–523.

Lugolobi F., Kurtz A. C. and Derry L. A. (2010) Germanium–silicon fractionation in a tropical, granitic weathering environment. *Geochim. Cosmochim. Acta* **74**, 1294–1308.

Mareschal L. (2008) Effet des substitutions d'essences forestières sur l'évolution des sols et de leur mineralogie. Ph. D. thesis, Université Henri Poincarré, Nancy-I, p. 324.

Mortlock R. A. and Froelich P. N. (1996) Determination of germanium by isotope dilution-hydride generation inductively coupled plasma mass spectrometry. *Anal. Chimica Acta* **322**, 5638–5645.

Murnane R. J. and Stallard R. F. (1990) Germanium and silicon in rivers of the Orinoco drainage basin. *Nature* **344**, 749–752.

Oliva P., Viers J., Dupré B., Fortuné J. P., Martin F., Braun J. J., Nahon D. and Robain H. (1999) The effect of organic matter on chemical weathering: study of a small tropical watershed: Nsimi-Zoétélé site, Cameroon. *Geochim. Cosmochim. Acta* **63**(23/24), 4013–4035.

Opfergelt S., Cardinal C., Henriet C., Draye X., André L. and Delvaux B. (2006a) Silicon isotope fractionation by banana (*Musa* spp.) grown in a continuous nutrient flow device. *Plant Soil* **285**, 333–345.

Opfergelt S., Cardinal D., Henriet C., André L. and Delvaux B. (2006b) Silicon isotope fractionation between plant parts in banana: In situ vs. In vitro. *J. Geochem. Explor.* **88**, 224–227.

Opfergelt S., Delvaux B., André L. and Cardinal D. (2008) Plant silicon isotopic signature might reflect soil weathering degree. *Biogeochemistry* **91**, 163–175.

Opfergelt S., de Bournonville G., Cardinal D., André L., Delstanche S. and Delvaux B. (2009) Impact of soil weathering degree on silicon isotopic fractionation during adsorption onto iron oxides in basaltic ash soils, Cameroon. *Geochim. Cosmochim. Acta* **73**, 7226–7240.

Opfergelt S., Cardinal D., André L., Delvigne C., Bremond L. and Delvaux B. (2010) Variations of δ^{30}Si and Ge/Si with weathering and biogenic input in tropical basaltic ash soils under monoculture. *Geochim. Cosmochim. Acta* **74**, 225–240.

Parkhurst D. L. and Appelo C. A. J. (1999) User's guide to PHREEQC (Version 2)—A computer program for speciation, batch-reaction, one-dimensional transport, and inverse geochemical calculations: U.S. Geological Survey Water-Resources Investigations Report 99-4259, p. 310.

Peel M. C., Finlayson B. L. and McMahon T. A. (2007) Updated world map of the Köppen-Geiger climate classification. *Hydrol. Earth Syst. Sci.* **11**, 1633–1644.

Pokrovski G. S., Martin F., Hazemann J.-L. and Schott J. (2000) An X-ray absorption fine structure spectroscopy study of germanium–organic ligand complexes in aqueous solution. *Chem. Geol.* **163**, 151–165.

Ranger J. (Ed), Andreux F. (Ed), Bienaime S., Berthelin J., Bonnaud P., Boudot J.P., Brechet C., Buee M., Calmet J.P., Chaussod R., Gelhaye D., Gelhaye L., Gerard F., Jaffrain J., Lejon D., Le Tacon F., Leveque J., Maurice J. P., Merlet D., Moukoumi J., Munier-Lamy C., Nourrisson G., Pollier B., Ranjard L., Simonsson M., Turpault M. P., Vairelles D., Zeller B. (2004) Effet des substitutions d'essence sur le fonctionnement organo-minéral de l'écosystème forestier, sur les communautés microbiennes et sur la diversité des communautés fongiques mycorhiziennes et saprophytes (cas du dispositif experimental de Breuil – Morvan). Rapport final du contrat INRA-GIP Ecofor 2001-24, n°INRA 1502A Nancy: INRA-Champenoux, Biogéochimie des écosystèmes forestiers, p. 202.

Reynolds B. C., Aggarwal J., André L., Baxter D., Beucher C., Brzezinski M. A., Engström E., Georg B., Land M., Leng M. J., Opfergelt S., Rodushkin I., Sloane H. J., Van den Boorn S. H. J. M., Vroon P. Z. and Cardinal D. (2007) An inter-laboratory comparison of Si isotope reference materials. *J. Anal. Atom. Spectrom.* **22**, 561–568.

Robert M. and Tessier D. (1974) Méthode de préparation des argiles des sols pour des études minéralogiques. *Ann. Agron.* **25**, 859–882.

Rouiller J., Burtin G. and Souchier B. (1972) La dispersion des sols dans l'analyse granulométrique. Méthode utilisant les résines échangeuses d'ions. *ENSAIA Nancy* **14**, 194–205.

Scribner A. M., Kurtz A. C. and Chadwick O. A. (2006) Germanium sequestration by soil: Targeting the roles of secondary clays and Fe-oxyhydroxides. *Earth Planet. Sci. Lett.* **243**, 760–770.

Smetacek V. (1999) Diatoms and the ocean carbon cycle. *Protist* **150**, 25–32.

Sommer M., Kaczorek D., Kuzyakov Y. and Breuer J. (2006) Silicon pools and fluxes in soils and landscapes-a review. *J. Plant Nutr. Soil Sci.* **169**, 310–329.

Tréguer P., Nelson D. M., Van Bennekom A. J., De Master D. J., Leynaert A. and Quéguiner B. (1995) The silica balance in the world ocean: a reestimate. *Science* **268**, 375–379.

Volk T. (1987) Feedbacks between weathering and atmospheric CO_2 over the last 100 million years. *Am. J. Sci.* **287**, 763–779.

Wedepohl K. H. (1995) The composition of the continental crust. *Geochim. Cosmochim. Acta* **59**, 1217–1232.

Yeghicheyan D., Carignan J., Valladon M., Bouhnik Le Coz M., Le Cornec F., Castrec-Rouelle M., Robert M., Aquilina L., Aubry E., Churlaud C., Dia A., Deberdt S., Dupré B., Freydier R., Gruau G., Hénin O., de Kersabiec A.-M., Macé J., Marin L., Morin N., Petitjean P. and Serrat E. (2001) A compilation of silicon and thirty one trace elements measured in the natural river water reference material SLRS-4 (NRC–CNRC). *Geostand. Newsl.* **25**, 465–474.

Ziegler K., Chadwick O. A., Brzezinski M. A. and Kelly E. F. (2005a) Natural variations of δ^{30}Si ratios during progressive basalt weathering, Hawaiian Islands. *Geochim. Cosmochim. Acta* **69**, 4597–4610.

Ziegler K., Chadwick O. A., White A. F. and Brzezinski M. A. (2005b) δ^{30}Si systematics in a granitic saprolite, Puerto Rico. *Geology* **33**, 817–820.

Associate editor: Martin Novak